Peri-Implant Bone Organization Under Immediate Loading State. Circularly Polarized Light Analyses: A Minipig Study

Jörg Neugebauer,* Tonino Traini,† Ulf Thams,‡ Adriano Piattelli,† and Joachim E. Zöller*

Background: Immediate loading of dental implants is currently one of the most examined topics in implant dentistry. Using screw implants with a microstructured surface and bone-quality–adapted insertion procedures, osseointegration is achieved when implants are initially stable and when splinted with the superstructure. Despite reported success, there is a shortage of information relating to remodeling and peri-implant bone formation with immediately loaded implants.

Methods: Four to six immediately loaded and unloaded dental implants with a microstructured surface were placed in the mandible and the maxilla in seven minipigs. A total of 85 implants were placed. After a 4-month healing period, all implants were retrieved. Histomorphometry was performed using a light microscope in transmitted polarized light connected to a high-resolution video camera interfaced to a monitor and personal computer. This optical system was associated with a digitizing pad and a histomorphometry software package with image capturing capabilities.

Results: Implants showed osseointegration if the average insertion torque of the implants within one bridge was >35 Ncm. If the primary stability of the bridge was <35 Ncm, all implants in the quadrant were lost after 4 months. The multivariate discriminant analysis showed the highest correlation for implant stability by bridge insertion torque (BIT), localization (mandible or maxilla), and implant insertion torque (IIT) as success parameters. The loaded implants displayed collagen fibers, which were oriented in a more transverse way. In addition, a higher quantity of secondary osteons was present. In comparison, the unloaded implants had collagen fibers with a more parallel orientation, and a higher quantity of marrow spaces was present.

Conclusions: When observed after 4 months, immediately loaded implants showed a higher degree of bone formation and remodeling in comparison to unloaded implants. Immediately loaded implants also demonstrated a prevalence of transversely oriented collagen fibers in the peri-implant bone. In this animal model, an average insertion torque of the implants within one bridge >35 Ncm was associated with the most successful implants. *J Periodontol 2006;77:152-160.*

KEY WORDS

Birefringence; collagen; dental implants; microscopy, polarization; osseointegration.

* Department of Craniomaxillofacial and Plastic Surgery, University of Cologne, Cologne, Germany.
† Dental School, University of Chieti-Pescara, Chieti, Italy.
‡ Department of Animal Pathology II, University Complutens Madrid, Madrid, Spain.

Immediate loading has recently become one of the most frequently recognized research topics in restorative dentistry. Following the developments of the immediate loading concept by Ledermann et al.,[1,2] a variety of related clinical approaches have been reported.[3-5]

The main objective of immediate loading is to achieve a high mechanical stability to avoid micromovements during the course of osseointegration.[6] For example, the standard implant placement procedure in areas of weak bone quality with lower success rates[7] was modified via undersized preparation to achieve high primary stability.[8] The osteotome technique was developed to increase the stability of implants[9] and to improve implant success.[10] A histologic study in rabbits showed that the microfractures, which occurred due to the bone condensing technique, improved the peri-implant bone formation in the first weeks after implant placement through the release of cytokines.[11] However, it is important to note that intensive use of the osteotomy technique can also harm the bone, with an increased crestal bone resorption.[12]

doi: 10.1902/jop.2006.040360

Although immediate loading significantly advanced the field of implant dentistry,[13] the implant surface still needed to be improved.[14] The commonly used titanium plasma-sprayed (TPS)–coated implants created a very high friction in dense bone. Histologic findings showed a wear of titanium with foreign body reactions.[15] In 1988, the first grit-blasted and etched implant surface was developed to enhance the Ledermann concept.[1] The subsequent surface treatments decreased healing time as well. The double-etched surfaces reduced the healing period to 8 weeks,[16] and the sand-blasted acid-etched (SLA)–type surfaces decreased healing time to as little as 6 weeks.[17] The rough surfaces improved the *de novo* bone formation due to the early adhesion of non-collagen proteins, such as osteopontin and bone sialoprotein, at the micropits.[18] Calcium phosphate nucleation at the calcium binding sites on these proteins continues the process of osseointegration, which culminates in crystal growth and collagen production with mineralization.[19]

The development of mineralized bone at the interface of immediately loaded implants depends on two key factors. First, the implant's mechanical aspects must avoid micromovements and create a static environment for the healing bone. Second, the appropriate biologic principles must be employed to avoid the formation of connective tissue and to achieve close bone-to-implant contact.[20-22]

In the mandible, no differences in the quality of bone formation around immediately loaded and unloaded implants have been found.[23] The present study aimed to further investigate mandible implantation through histologic and statistical evaluation, while also continuing to explore differences found in the maxilla for the above-mentioned study.[23] In doing so, circularly polarized light (CPL) was used to study the orientation of the collagen fibers and to determine the quality of bone remodeling.[24] This method is effective in demonstrating differences in bone formation, as linear light vibrates in all planes, while the polarized light vibrates in only one plane. In a linear polarizing light microscope, normal light is first passed through a polarizing filter and then through the microscope stage onto a similar filter. This filter is called an analyzer and has a transmission axis that rotates to form a 90° angle with the polarizer. If no specimen is present between the polarizer and the analyzer, no light can pass though the cross-polars to the eye piece. This point is called the angle of extinction. However, if a birefringence material is placed between the cross-polars, the light interacts with the molecular organization of the material. The light undergoes a phase shift or causes a rotation of the electromagnetic vector, which vibrates in a plane different from its original polarization.[24] The material then becomes visible at the eyepiece. Circularly polarized light microscopy does not produce the characteristic extinction angle points but, instead, illuminates all of the fibers nearly equally, regardless of their orientation. The lack of directional specificity in illuminating collagen fibers makes circularly polarized light an ideal image processing technique that can be used to quantify the collagen's fiber content and the fiber orientation.[24]

Determining the orientation of the collagen fibers was important for this study because it enabled evaluation of the quality of osseointegration and bone remodeling on immediately loaded and non-loaded implants.

The aim of this study was to analyze the course of osseointegration for immediately loaded implants in the posterior arch of the mandible and maxilla in minipigs. The implants used had a grit-blasted and high-temperature etched surface. The implant design allowed a condensation effect through standardized undersized implant side preparation in trabecular bone.

MATERIALS AND METHODS

The study protocol was approved by the Institutional Animal Care Committee of the Military Hospital General Gomez-Roman, Madrid, Spain. Seven adult male Göttingen minipigs (18 to 21 months old; average weight, 35 kg) were given general anesthesia, which was maintained by halothane 2% in an oxygen/nitrous oxide mixture (1:1).§ To secure normal blood gases, the animals were artificially ventilated with a minute volume of 150 ml/kg body weight/minute. Once the animals were anesthetized, an impression of the dentition, which had to be extracted, was taken. Vacuum-formed templates were created for the later surgical and prosthetic procedure. The premolars and molars in the mandible and maxilla were then extracted. For five animals, extractions were performed only on the contralateral side, and a natural dentition provided the implant load. Two animals received extraction in all quadrants, and implant-borne bridges constituted the loading.

Three months after tooth extraction, implant placement and immediate prosthetic reconstruction were performed in sterile conditions while the minipigs were under general anesthesia. An antibiotic, benzylpenicillin/dihydrostreptomycin,‖ was administered subcutaneously at 0.5 ml/kg body weight every 48 hours for 7 days. An analgesic, buprenorphine,¶ was injected intramuscularly at 0.05 mg/kg body weight every 12 hours for 3 days. The mucosa was rinsed with 0.2% chlorhexidine gluconate.# After a crestal incision, a mucoperiosteal flap was raised. The implant sites were sequentially enlarged to 3.8 mm

§ Linde, Höllriegelskreuth, Germany.
‖ Tardomycel, BayerVital, Leverkusen, Germany.
¶ Temgesic, Boehringer, Mannheim, Germany.
# Doreperol N, Dr. Rentschler Arzneimittel, Laupheim, Germany.

in diameter with pilot and spiral drills according to the standard protocol of the manufacturer.** The bone quality was determined during the initial preparation.[25] The crestal preparation was performed in cortical bone (Classes 1 and 2) up to a depth of 5 mm. In spongy areas, crestal preparation reached a depth of 2 mm in bone density Class 4 and 4 mm in bone density Class 3. To avoid crestal bone resorption even in spongy bone, a short crestal preparation was performed so that the internal condensation effect with higher crestal bone resorption was not overemphasized. In weaker bone sites, a systematic undersized preparation was performed to achieve a higher mechanical stabilization. Between four and six implants were inserted in each surgical side. The implants used were cylindrical, self-tapping, and screw shaped.†† The implants were 3.8 mm in diameter and 11 mm in length and processed.‡‡ A total of 85 implants were placed. Each implant was placed,§§ and the required insertion torque was documented as the implant insertion torque (IIT) (Fig. 1). The control implants were placed in the anterior, remained unloaded, and were submerged. Due to the predicted course of healing of the submerged implants, only one control implant was placed per surgical side. The wound was closed with bioabsorbable sutures‖‖ (Fig. 2). At the end of surgery, fiber-reinforced bridges were placed on four to five distal implants. The prefabricated temporary abutment caps¶¶ were positioned on the temporary abutments (Fig. 3). Fiber-reinforced strips## were used to connect the temporary abutment caps. The vacuum-formed templates were filled with temporary acrylic*** and positioned over the temporary abutment caps. Saline irrigation was used to cool the resin during the polymerization period. Subsequently, the superstructure was removed and contoured. The interproximal spaces were created at least 2 mm wide to prevent pressure on the mucosa during postoperative swelling. The bridges were installed with zinc-phosphate cement††† (Fig. 4). Intraoral adjustments were performed to eliminate any direct occlusal contact. A follow-up examination was carried out 1 and 2 months after surgery. The minipigs were sedated to check if the provisional restorations were still in service or had been lost. Starting on the 14th postoperative day, polychromatic intravital fluorescence

Figure 1.
Placement of cylindrical implant in maxilla.

Figure 2.
Situation after placement of four implants prior to prosthetic rehabilitation.

Figure 3.
Splinting of implants with caps and strips.

** Friadent, Mannheim, Germany.
†† XiVE, Friadent.
‡‡ Friadent plus surface, Friadent.
§§ FRIOS Unit S, Friadent.
‖‖ Vicryl 2-0, Ethicon, Norderstedt, Germany.
¶¶ Palavit G, Heraeus Kulzer, Wehrheim, Germany.
FibreKor, Jeneric/Pentron, Wallingford, CT.
*** Protemp Garant, ESPE Dental, Seefeld, Germany.
††† Harvard Cement, Richter & Hoffmann Dental-Gesellschaft, Berlin, Germany.

Figure 4.
Finalized bridge.

labeling was performed. The sequential administrations of fluorescent dyes allowed us to follow the direction and the topographic localization of new bone formation. The fluorescent dyes were incorporated into the mineralization matrix through chelation.[26]

The fluorescent bone markers used in the study were oxytetracycline‡‡‡ (15 mg/kg body weight), alizarine-complexon§§§ (30 mg/kg body weight), and xylenol orange‖‖‖ (90 mg/kg body weight). Each marker was administered via intramuscular injections of the fluorescent dyes in 2% $NaHCO_3$ solution. At the end of the 4-month healing period, the minipigs were sacrificed by means of induced cardiac arrest via intravenous injection of a 20% solution of pentobarbital.¶¶¶ The 4-month healing period was chosen to allow time for complete osseointegration of the implants. After this time, first signs of remodeling were expected. The implants were removed together with the surrounding bone and fixed in Schaffer's solution (two parts 96% ethanol and one part 37% formaldehyde) for 24 hours. The specimens were dehydrated in a graded series of ethanol and then embedded in methylmethacrylate.### The samples were cut parallel to the longitudinal axis of the implant in an orovestibular direction. Via the sawing and grinding technique,[26] the samples were ground to a thickness of 100 μm.****

Histomorphometry was performed using a light microscope†††† in transmission light at a magnification of 10-fold. The microscope was connected to a high-resolution video camera‡‡‡‡ and interfaced to a monitor and personal computer.§§§§ This optical system also used a digitizing pad‖‖‖‖ and a histomorphometry software package¶¶¶¶ with image capturing capabilities. To measure the differences in collagen fiber orientation, two central sections from 10 randomly selected loaded implants (five in the mandible and five in the maxilla) and 10 randomly chosen unloaded implants (five in the mandible and five in the maxilla) were taken. Sections were ground to a final thickness of 100 ± 5 μm (mean ± SD). The sections were mounted on glass slides and observed under CPL at magnification ×50 using an optical microscope. The areas of analyses were standardized for all specimens. This was accomplished through the use of a mirror image technique that generated and superimposed a grid of 350,000 square pixels onto the bone adjacent to each side of the implant's section. CPL was generated by combining a quarter-wave retarder and two polarizing filters. One circular polarizing filter was placed beneath the glass and directly below the specimen. The other filter was positioned above the specimen on the superior end of the objective. Concurrently, a quarter-wave retarder was placed just below the analyzer. In contrast to plane polarized light, CPL microscopy does not produce characteristic extinction points but, rather, illuminates all fibers nearly equally, regardless of their orientation. To view the collagen fiber orientation, different levels of resolution were needed. These levels were achieved by rotating the analyzer at –5° and the quarter-wave retarder at +5° and vice versa for each image that was evaluated.

Eight images were evaluated for each specimen (two for each side of the section). All 320 digitized images for analysis were stored in TIFF format with $N \times M = 768 \times 1{,}024$ grid of pixels for a 24 bit. Each image was calibrated using the Pythagorean theorem for distance calibration, which reports the number of pixels between two selected points. The interthread's distance of 0.85 mm (tip to tip) was used, and a scale of 760.81 pixels/mm was used for calculating the calibration. Linear remapping of the pixel values was used to calibrate the intensity of images. All images were converted in gray scale at eight bits. Each pixel (specific cell in the grid) was assigned a value between 0 and 255 (0 = black; 255 = white). Image analysis software was used to quantify the birefringence; the black and white represented longitudinal and transverse collagen fibers, expressed by semiquantitative digital densitometry. The extension of the area relative to collagen fiber orientation was expressed in square pixels.

Statistical analyses were performed by a computer program.#### To determine the stability of the implants within one bridge, the average bridge insertion

‡‡‡ Fluka, Buchs, Switzerland.
§§§ Fluka.
‖‖‖ RdH Laborchemikalien, Seelze, Germany.
¶¶¶ Narcoren, Merial, Hallbergmoos, Germany.
Technovit 7200, Heraeus Kulzer.
**** Exakt Apparatebau, Norderstedt, Germany.
†††† Laborlux S, Leitz, Wetzlar, Germany.
‡‡‡‡ 3CCD, JVC KY-F55B JVC, Yokohama, Japan.
§§§§ Intel Pentium III 1200 MMX, Intel, Santa Clara, CA.
‖‖‖‖ Matrix Vision, GmbH, Oppenweiler, Germany.
¶¶¶¶ Image-Pro Plus 4.5, Media Cybernetics; Immagini & Computer, Milan, Italy.
SPSS for Windows 11.0, SPSS, Chicago, IL.

torque (BIT) was calculated and assigned to each implant. This number represented the sum of all insertion torques used for the implants in one bridge, divided by the number of implants in that bridge. Tukey box plots for visualizing the insertion torques were generated. Multivariate discriminant analysis was used to determine which variables contribute to implant success.

RESULTS

The method of preparation used for each receptor site was determined based on bone quality. Crestal drills were used in the mandible and bone condensing instruments in the maxilla, and 94.5% of all loaded implants (N = 69/73) were placed with an IIT >25 Ncm. The mean IIT was 33.46 ± 11.59 Ncm in the maxilla and 48.48 ± 11.24 Ncm in the mandible; the difference was statistically significant (*t* test; $P<0.000$). The mean value of the BIT was evaluated. The mean BIT was 34.21 ± 7.22 Ncm in the maxilla and 48.49 ± 5.92 Ncm in the mandible. This difference was statistically significant (*t* test; $P<0.000$). The details for the subgroups of loaded and unloaded implants are shown in Table 1. The box plot for the torque values (Fig. 5) showed a high variation of IIT and a lower BIT in the maxilla than in the mandible. The box plot (Fig. 6) for torque and success for the loaded implants showed that the failing implants (N = 27) had a lower BIT than the successful implants (N = 46).

The cross-table for BIT and implant success (Table 2) shows that the bridges were stable, and the implants obtained osseointegration if the BIT was >35 Ncm. The cross-table for BIT and jaw (Table 3) shows that the bridges in the maxilla mainly had a BIT <35 Ncm. In the maxilla, 25 of 34 implants failed. In the mandible, two of 39 implants failed. These two implants were still in place at implant retrieval. The applied insertion torque was very high in dense bone.

Table 1.

Torque Values for Loaded and Unloaded Implants

Prosthetic Loading		Implant Survival	N	Mean	SD	SE
Loaded	BIT	Success	46	47.61	6.398	1.943
		Failure	27	32.01	5.466	1.052
	IIT	Success	46	47.50	12.191	1.797
		Failure	27	32.04	10.942	2.106
Unloaded	IIT	Success	9	42.22	11.756	3.919
		Failure	3	35.00	15.000	8.660

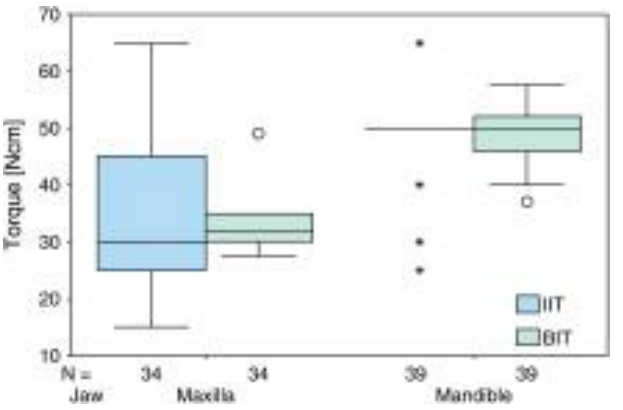

Figure 5.
*Box plot for insertion torque versus corresponding jaw (O = outlier values; * = extreme value).*

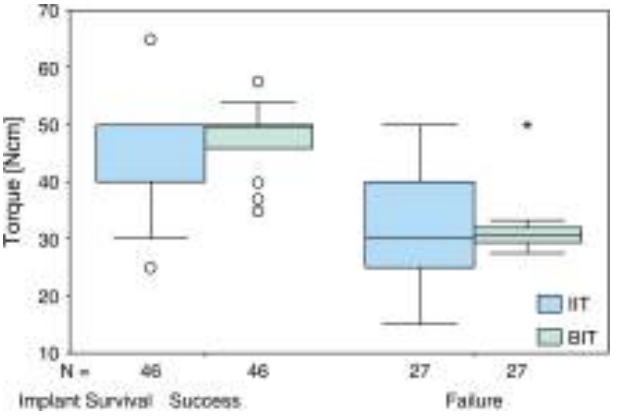

Figure 6.
*Box plot for insertion torque versus implant survival (O = outlier values; * = extreme value).*

A multivariate discriminant analysis for BIT, jaw, and IIT was performed to determine which variables contributed to implant success. Common correlation within the groups of the discriminated variables and the standardized discriminant function variable showed the highest correlation for BIT with 0.920, for jaw with 0.731, and for IIT with 0.472.

Under CPL, transverse collagen fibers, which lie in the plane of the section, appeared in yellow/orange, while longitudinal collagen fibers running perpendicular to the plane of the section appeared as a white/gray shade (Figs. 7 and 8). The area covered by transverse collagen fibers in the loaded implants was 112,453 ± 4,605 pixels (mean ± SD).[2] In the unloaded implants, transverse collagen fibers covered an area of only 87,256 ± 2,428 pixels (mean ± SD).[2] A significant difference in the amount of transversal fibers in loaded and unloaded implants could be found ($P<0.05$) (Table 4). In loaded implants, transverse

Table 2.

Cross-Table for BIT and Implant Survival

BIT (Ncm)	Implant Survival		Total Number of Implants
	Success	Failure	
28		3	3
29		4	4
30		3	3
31		6	6
32		6	6
33		3	3
35	3		3
37	3		3
40	5		5
46	6		6
49	6		6
50	13	2	15
54	6		6
58	4		4
Total	46	27	73

Table 3.

Cross-Table for BIT and Jaw

BIT (Ncm)	Jaw		Total
	Maxilla	Mandible	
28	3		3
29	4		4
30	3		3
31	6		6
32	6		6
33	3		3
35	3		3
37		3	3
40		5	5
46		6	6
49	6		6
50		15	15
54		6	6
58		4	4
Total	34	39	73

fibers were mainly associated with compression zones. These zones were primarily detected at the inferior part of the threads or the area of internal condensation between the crestal and apical thread. In the unloaded implants, transverse collagen fibers were randomly distributed in the peri-implant bone.

Due to the fact that implants with a 1.5-mm polished collar were used in the immediately loaded group, no bone-to-implant contact was found on the loaded implants. On the submerged implants, the bone-to-implant contact was higher on the smooth surface in comparison to the loaded implants.

DISCUSSION

Longitudinal studies[1,2,4,5] and recent reports[21,22,27-30] have confirmed that immediate loading is a safe and effective protocol for the anterior mandible. A main prerequisite for successful immediate loading is to avoid micromovements >100 μm.[6] The reported optimal insertion torques range from 40 to 72 Ncm[31-34] and apply to both multiple units and single crowns. Internal condensation methods have also been used to improve primary stability. In the maxilla, bone condensing has further been used to improve bone length and volume in the sinus area.[9,35] When performing bone condensation in the maxilla, BIT values ranged between 28 and 49 Ncm. In the mandible, the BIT values were between 37 and >50 Ncm. This implies that high insertion torque values are not always necessary for achieving osseointegration of immediately loaded implants.

In the present study, bridges with a BIT <35 Ncm failed, while bridges with BIT >35 Ncm were successful. Control implants in the mandible were completely osseointegrated. The multivariate discriminant analysis demonstrated that the BIT has more influence on implant success than IIT or jaw location. The present study has demonstrated that the average insertion torque of implants within a bridge functions as a parameter for predicting implant stability. This suggests that stabilization of a superstructure can enable even less stable implants to achieve osseointegration. High primary stability can also be achieved in the maxilla through application of bone condensing techniques[9,11,36,37] or implant cavity undersizing methods.[8] A high insertion torque can also lead to high resorption[12] and a loss of implants like that found in this study with the two failures in the mandible.

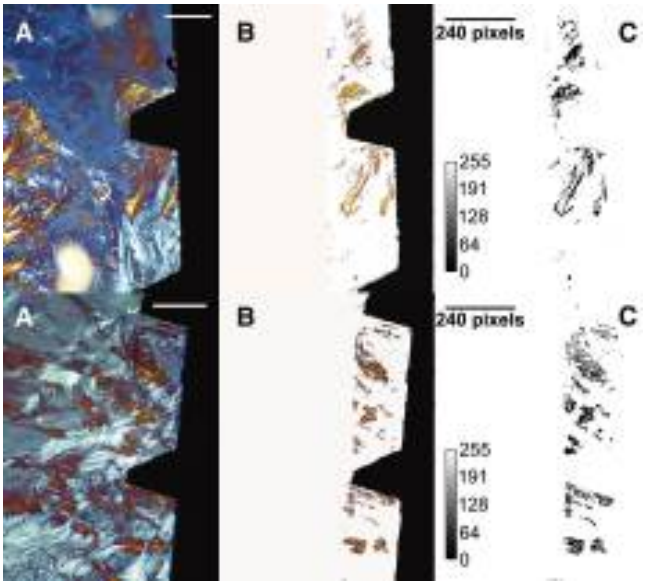

Figure 7.
*CPL of loaded implant with zone of transversal collagen fiber in yellow/orange **(A)**, mathematical separation of the measured area **(B)**, and threshold of image for calculation of corresponding pixels **(C)**. (Magnification ×50; bar in A = 0.25 mm.)*

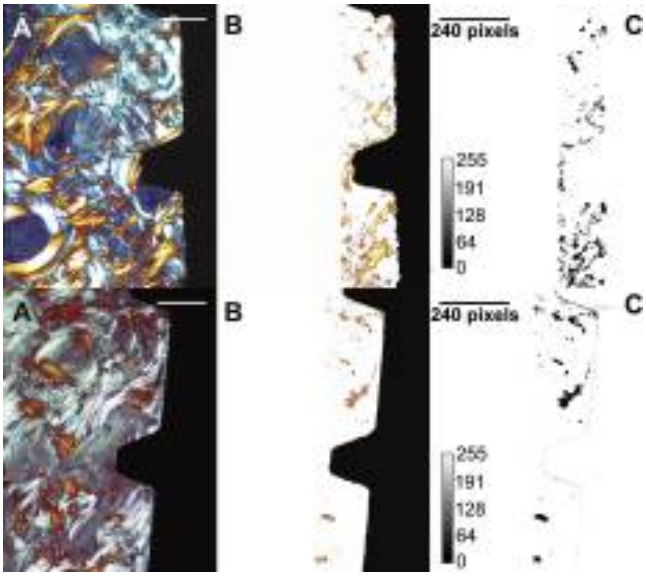

Figure 8.
*CPL of unloaded implant with zone of transversal collagen fiber in yellow/orange **(A)**, mathematical separation of the measured area **(B)**, and threshold of image for calculation of corresponding pixels **(C)**. (Magnification ×50; bar in A = 0.25 mm.)*

The course of osseointegration has been described for microstructured surfaces by Davies.[19] Microstructured implant surfaces improved initial bone healing by stabilizing the fibrin clot network. Microstructured surfaces have shown a higher success rate when compared to smooth or machined surfaces. Findings supporting these statements were derived from both clinical and in vitro studies.[38,39] Various surfaces have been tested for characteristics to improve the proliferation and differentiation of osteoblasts. Large-grit-blasted and high-temperature etched and SLA surfaces have shown the highest numbers of cells with total spreading at stage 4.[40] In terms of bone formation, the advantage of the large-grit-blasted and high-temperature etched surface in comparison to the TPS-coated implant was demonstrated in a study of periodontally infected sites for immediate implant placement. The large-grit-blasted and high-temperature etched surface showed more homogeneous bone formation in comparison to the TPS-coated implants.[41] A comparison study of four different implant designs with various surfaces with immediately loaded implants showed homogeneous results for the large-grit-blasted and high-temperature etched surface.[42]

Table 4.

Statistical Evaluation for Transverse Collagen Fiber Area in Peri-Implant Bone

Groups	Transverse Collagen Fibers (square pixel; mean ± SD)
Loaded (N = 160)	112,453 ± 4,605*
Unloaded (N = 160)	87,256 ± 2,428*
P value	<0.001

* Significantly different between loaded and unloaded groups (unpaired *t* test; $P < 0.05$).

The quality of osseointegration is also an important factor to consider. The quantity and orientation of the collagen fibers surrounding the implant can serve as a reliable measure of osseointegration quality. Recent literature has further reported the use of birefringence interpretation patterns for measuring and characterizing osseointegration. Black et al.[43,44] demonstrated that the birefringence pattern changes along the length of an osteon. However, opposing studies have questioned the fundamental interpretation of the birefringence pattern in bone. Investigators have also questioned the Gebhardt model,[45] which suggests that collagen fibers alternate between the longitudinal and transversal orientation in successive lamellae. Giraud-Guille[46] demonstrated that collagen fibrils could be distributed across certain bone lamellae in the form of a superimposed series of nested areas with variable angles.

Other researchers believe that lamellar structure is derived from variability in composition or density and not from collagen fiber orientation.[47] The classification of the osteons could depend on the orientation of the collagen fibers.[24] The goal of the present article was

not to argue these issues but simply to present relating data that were obtained using the birefringence method.

Numerous studies have reported that bone loss around implants is greatest during healing and the first year of function,[48-50] regardless of implant design. Factors causing bone loss vary among surgical trauma, occlusal overload, biologic width,[51] and inadequate stress at the implant–bone interface.[52-54] By directly observing the microstructure of peri-implant bone, the present study has indicated inadequate bone as a causal factor for bone loss. The implant profile, at both microscopic and macroscopic levels, is the main distributor of stress to the bone. Strain is concentrated at the point where bone contacts the top radius of the thread. Vaillancourt et al.[53] reported an upper limit of the disuse range at 1.6 Mpa. According to the $\varepsilon = \sigma/E$ relation, that corresponds to a microstrain of 137 $\mu\varepsilon$/360 $\mu\varepsilon$ depending on the bone's modulus of elasticity chosen. According to Frost,[55] 1,500 to 2,500 $\mu\varepsilon$ is the range of "minimum effective strain for mechanically controlled bone remodeling," and a strain of 4,000 $\mu\varepsilon$ will inhibit the bony structure from adapting or repairing itself. Therefore, a creep phenomena and fatigue flaw will evolve.[56]

The present study found that appropriate primary stability and limited micromovement of immediately loaded implants could be achieved in the posterior arch. The self-tapping screw implants used in this study osseointegrated and showed a high degree of remodeling under immediate loading conditions. Past studies have documented that immediate loading can only be achieved in the anterior mandible. However, because these studies limited their focus to certain jaw locations and maintained primary stability only in good bone quality, the full scope of areas suitable for immediate loading cannot be confirmed. A key significant finding of the present study was that mechanical loading throughout the course of osseointegration led to earlier formation and increased quantity of transversely oriented collagen fibrils.

REFERENCES

1. Ledermann PD. The new Ledermann screw (in German). *Quintessenz* 1988;39:799-815.
2. Ledermann PD, Schenk RK, Buser D. Long-lasting osseointegration of immediately loaded, bar-connected TPS screws after 12 years of function: A histologic case report of a 95-year-old patient. *Int J Periodontics Restorative Dent* 1998;18:552-563.
3. Becker W, Becker BE, Huffstetlert S. Early functional loading at 5 days for Brånemark implants placed into edentulous mandibles: A prospective, open-ended, longitudinal study. *J Periodontol* 2003;74:695-702.
4. Chiapasco M, Gatti C. Implant-retained mandibular overdentures with immediate loading: A 3- to 8-year prospective study on 328 implants. *Clin Implant Dent Relat Res* 2003;5:29-38.
5. Chiapasco M, Gatti C, Rossi E, Haefliger W, Markwalder TH. Implant-retained mandibular overdentures with immediate loading. A retrospective multicenter study on 226 consecutive cases. *Clin Oral Implants Res* 1997;8:48-57.
6. Brunski JB. Avoid pitfalls of overloading and micromotion of intraosseous implants. *Dent Implantol Update* 1993;4:77-81.
7. Jaffin RA, Berman CL. The excessive loss of Brånemark fixtures in type IV bone: A 5-year analysis. *J Periodontol* 1991;62:2-4.
8. Horiuchi M, Ichikawa T, Kanitani HR, Kawamoto N, Matsumoto N. Pilot-hole preparation for proper implant positioning and the enhancement of bone formation. *J Oral Implantol* 1995;21:318-324.
9. Summers RB. A new concept in maxillary implant surgery: The osteotome technique. *Compendium* 1994; 15:152, 154-156, 158 passim; quiz 162.
10. Piattelli A, Trisi P, Romasco N, Emanuelli M. Histologic analysis of a screw implant retrieved from man: Influence of early loading and primary stability. *J Oral Implantol* 1993;19:303-306.
11. Nkenke E, Kloss F, Wiltfang J, et al. Histomorphometric and fluorescence microscopic analysis of bone remodelling after installation of implants using an osteotome technique. *Clin Oral Implants Res* 2002;13:595-602.
12. Strietzel FP, Nowak M, Kuchler I, Friedmann A. Periimplant alveolar bone loss with respect to bone quality after use of the osteotome technique: Results of a retrospective study. *Clin Oral Implants Res* 2002;13: 508-513.
13. Salama H, Rose LF, Salama M, Betts NJ. Immediate loading of bilaterally splinted titanium root-form implants in fixed prosthodontics – A technique reexamined: Two case reports. *Int J Periodontics Restorative Dent* 1995;15:344-361.
14. Krafft T, Peschla M. Abrasion of surface components in endosseous implants depending on their shape and coating. *Int J Oral Maxillofac Surg* 1994;23:418-419.
15. Schliephake H, Reiss G, Urban R, Neukam FW, Guckel S. Metal release from titanium fixtures during placement in the mandible: An experimental study. *Int J Oral Maxillofac Implants* 1993;8:502-511.
16. Lazzara RJ, Porter SS, Testori T, Galante J, Zetterqvist L. A prospective multicenter study evaluating loading of Osseotite implants two months after placement: One-year results. *J Esthet Dent* 1998;10:280-289.
17. Buser D, Nydegger T, Hirt HP, Cochran DL, Nolte LP. Removal torque values of titanium implants in the maxilla of miniature pigs. *Int J Oral Maxillofac Implants* 1998;13:611-619.
18. Davies JE. In vitro modeling of the bone/implant interface. *Anat Rec* 1996;245:426-445.
19. Davies JE. Mechanisms of endosseous integration. *Int J Prosthodont* 1998;11:391-401.
20. Frost HM. The biology of fracture healing. *Clin Orthop* 1989;248:283-293.
21. Piattelli A, Corigliano M, Scarano A, Costigliola G, Paolantonio M. Immediate loading of titanium plasma-sprayed implants: A histologic analysis in monkeys. *J Periodontol* 1998;69:321-327.
22. Piattelli A, Paolantonio M, Corigliano M, Scarano A. Immediate loading of titanium plasma-sprayed screw-shaped implants in man: A clinical and histological report of two cases. *J Periodontol* 1997;68:591-597.
23. Nkenke E, Lehner B, Weinzierl K, et al. Bone contact, growth, and density around immediately loaded implants in the mandible of mini pigs. *Clin Oral Implants Res* 2003;14:312-321.

24. Bromage TG, Goldman HM, McFarlin SC, Warshaw J, Boyde A, Riggs CM. Circularly polarized light standards for investigations of collagen fiber orientation in bone. *Anat Rec B New Anat* 2003;274:157-168.
25. Misch CE. Density of bone: Effect on treatment plans, surgical approach, healing, and progressive bone loading. *Int J Oral Implantol* 1990;6:23-31.
26. Becker J, Meissner T, Neukam FW, Knöfler W, Graf H-L, Reichart P. Animal experimental investigation for the healing of ANOF-coated titanium implants (in German). *Z Zahnärztl Implantol* 1991;7:162-169.
27. Calvo MP, Muller E, Garg AK. Immediate loading of titanium hexed screw-type implants in the edentulous patient: Case report. *Implant Dent* 2000;9:351-357.
28. Degidi M, Petrone G, Iezzi G, Piattelli A. Histologic evaluation of a human immediately loaded titanium implant with a porous anodized surface. *Clin Implant Dent Relat Res* 2002;4:110-114.
29. Degidi M, Piattelli A. Immediate functional and non-functional loading of dental implants: A 2- to 60-month follow-up study of 646 titanium implants. *J Periodontol* 2003;74:225-241.
30. Lorenzoni M, Pertl C, Zhang K, Wegscheider WA. In-patient comparison of immediately loaded and non-loaded implants within 6 months. *Clin Oral Implants Res* 2003;14:273-279.
31. Calandriello R, Tomatis M, Rangert B. Immediate functional loading of Brånemark System implants with enhanced initial stability: A prospective 1- to 2-year clinical and radiographic study. *Clin Implant Dent Relat Res* 2003;5(Suppl. 1):10-20.
32. Hui E, Chow J, Li D, Liu J, Wat P, Law H. Immediate provisional for single-tooth implant replacement with Brånemark system: Preliminary report. *Clin Implant Dent Relat Res* 2001;3:79-86.
33. Lorenzoni M, Pertl C, Zhang K, Wimmer G, Wegscheider WA. Immediate loading of single-tooth implants in the anterior maxilla. Preliminary results after one year. *Clin Oral Implants Res* 2003;14:180-187.
34. Wohrle PS. Single-tooth replacement in the aesthetic zone with immediate provisionalization: Fourteen consecutive case reports. *Pract Periodontics Aesthet Dent* 1998;10:1107-1114.
35. Summers RB. The osteotome technique: Part 3 – Less invasive methods of elevating the sinus floor. *Compendium* 1994;15:698, 700, 702-694 passim; quiz 710.
36. Abels N, Schiel HJ, Hery-Langer G, Neugebauer J, Engel M. Bone condensing in the placement of endosteal palatal implants: A case report. *Int J Oral Maxillofac Implants* 1999;14:849-852.
37. Summers RB. The osteotome technique: Part 2 – The ridge expansion osteotomy (REO) procedure. *Compendium* 1994;15:422, 424, 426, passim; quiz 436.
38. Rupp F, Scheideler L, Rehbein D, Axmann D, Geis-Gerstorfer J. Roughness induced dynamic changes of wettability of acid etched titanium implant modifications. *Biomaterials* 2004;25:1429-1438.
39. Lumbikanonda N, Sammons R. Bone cell attachment to dental implants of different surface characteristics. *Int J Oral Maxillofac Implants* 2001;16:627-636.
40. Sammons RL, Lumbikanonda N, Gross M, Cantzler P. Comparison of osteoblast spreading on microstructured dental implant surfaces and cell behaviour in an explant model of osseointegration. A scanning electron microscopic study.*Clin Oral Implants Res* 2005;16:657-666.
41. Novaes AB, Papalexiou V, Grisi MF, Souza SS, Taba M, Kajiwara JK. Influence of implant microstructure on the osseointegration of immediate implants placed in periodontally infected sites. *Clin Oral Implants Res* 2004;15:34-43.
42. Weinländer M, Neugebauer J, Lekovic V, Zoeller JE, Vasilic N, Plenk H Jr. Mechanical stability and histological analysis of immediate loaded implants with various surfaces and designs. *Clin Oral Implants Res* 2003;14:312-321.
43. Black J, Mattson R, Korostoff E. Haversian osteons: Size, distribution, internal structure, and orientation. *J Biomed Mater Res* 1974;8:299-319.
44. Black J, Mattson RU. Relationship between porosity and mineralization in the Haversian osteon. *Calcif Tissue Int* 1982;34:332-336.
45. Gebhardt W. Functional configuration of fine and coarse structure elements of bone in vertebrae II special part structure of the haversian lamella and its functional relevance (in German). *Arch Entwickler Mech Org* 1906;20:187-322.
46. Giraud-Guille MM. Twisted plywood architecture of collagen fibrils on human compact bone osteons. *Calcif Tissue Int* 1988;42:167-180.
47. Marotti G. A new theory of bone lamellation. *Calcif Tissue Int* 1993;53(Suppl. 1):S47-56.
48. Gomez-Roman G, Schulte W, d'Hoedt B, Axman-Krcmar D. The Frialit-2 implant system: Five-year clinical experience in single-tooth and immediately postextraction applications. *Int J Oral Maxillofac Implants* 1997;12:299-309.
49. Proussaefs P, Kan J, Lozada J, Kleinman A, Farnos A. Effects of immediate loading with threaded hydroxyapatite-coated root-form implants on single premolar replacements: A preliminary report. *Int J Oral Maxillofac Implants* 2002;17:567-572.
50. Rocci A, Martignoni M, Gottlow J. Immediate loading of Brånemark System TiUnite and machined-surface implants in the posterior mandible: A randomized open-ended clinical trial. *Clin Implant Dent Relat Res* 2003;5(Suppl. 1):57-63.
51. Oh TJ, Yoon J, Misch CE, Wang HL. The causes of early implant bone loss: Myth or science? *J Periodontol* 2002;73:322-333.
52. Mihalko WM, May TC, Kay JF, Krause WR. Finite element analysis of interface geometry effects on the crestal bone surrounding a dental implant. *Implant Dent* 1992;1:212-217.
53. Vaillancourt H, Pillar R, McCammond D. Finite element analysis of bone remodeling around porous-coated dental implants. *J Appl Biomater* 1995;6:267-282.
54. Wiskott HW, Belser UC. Lack of integration of smooth titanium surfaces: A working hypothesis based on strains generated in the surrounding bone. *Clin Oral Implants Res* 1999;10:429-444.
55. Frost HM. Vital biomechanics: Proposed general concepts for skeletal adaptations to mechanical usage. *Calcif Tissue Int* 1988;42:145-156.
56. Isidor F. Loss of osseointegration caused by occlusal load of oral implants. A clinical and radiographic study in monkeys. *Clin Oral Implants Res* 1996;7:143-152.

Correspondence: Prof. Adriano Piattelli, Dental School, University of Chieti-Pescara, Via F. Sciucchi 63, 66100 Chieti, Italy. Fax: 39-0871-3554076; e-mail: apiattelli@unich.it.

Accepted for publication June 14, 2005.